Amina ECHCHAACHOUAI[1], Soumia EL HANI[1], Ahmed HAMMOUCH[2]

Department of Electrical engineering, ENSET Rabat, Mohammed V University, Rabat, Morocco (1), National Center for Scientific and Technical Research, Rabat, Morocco (2)

doi:10.15199/48.2018.03.04

Comparison of three estimators used in a sensorless MPPT strategy for a wind energy conversion chain based on a PMSG

Abstract. *In this paper a WECS (Wind Energy Conversion System) based on a PMSG (Permanent Magnet Synchronous Generator) and implementing a sensorless MPPT (Maximum Power Point Tracking) strategy is presented using three types of generator rotor speed and angle estimators; the Angle Tracking Observer, the Extended Kalman Filter and the Synchronous Reference Frame Phase Locked Loop. The main purpose is to compare these estimators. Simulation results in Matlab-Simulink allowing this comparison can be found at the end of this work.*

Streszczenie. *W artykule opisano generator z magnesami stałymi PMSG wykorzystujący strategię MPPT (śledzenie maksimum mocy). Porównano trzy typy estymatorów prędkości i kąta obrotu wirnika: czujnik kąta obrotu (angle tracking observer), filtr Kalmana i synchroniczną pętlę fazową (synchronous frame phase locked loop).* ***Porównanie trzech estymatorów wykorzystywanych w strategii śledzenia maksimum mocy MPPT w generatorze synchronicznym z magnesami trwałymi PMSG***

Słowa kluczowe: generator synchroniczny z magnesami trwałymi PMSG, bezczujnikowe śledzenie maksimum mocy MPPT
Keywords: WECS, Direct-drive PMSG, sensorless MPPT, SRF-PLL, EKF, ATO, FOC, Extremum seeking

Introduction

Wind energy is one of the prominent renewable energy sources on earth. The global trend of recent research in this field is to minimize the overall cost of the Wind Energy Conversion System (WECS) while improving the quality of the produced power. With this aim, several works have been carried out to avoid the use of the mechanical sensors which are expensive to buy and maintain. The principal role of the sensors is measuring the generator rotation speed as well as the angle of the rotor that are necessary for the control of the system and the search of the maximum points of the extractable power. Reliability of the variable speed wind turbine can be improved significantly using a direct-drive Permanent Magnet Synchrounous Generator (PMSG) [1].

A sensorless Maximum Power Point Tracking (MPPT) strategy is proposed to control the pre-mentioned structure, it consists of two levels; the first is a power regulation loop generating the reference value of current i_{qref} to the Field Oriented Control (FOC) [2] justified by a power maximization analysis. The second level is the extremum seeking method [3] generating the optimum value of the coefficient including turbine parameters in the expression of the turbine output power.

The main objective of this paper is to compare three types of estimators used to build the sensorless MPPT. The first estimator is an Angle Tracking observer (ATO) [4], the second is the Extended Kalman Filter (EKF) [5] and the third is the Synchronous Reference Frame Phase Locked Loop (SRF-PLL) [6]. The global wind conversion chain is presented in Fig.1.

Simulation results obtained using Matlab-Simulink and allowing the comparison of the three estimators can be found at the end of this paper. In the conclusion we evaluate performance of the three estimators and give their basic advantages and disadvantages.

Global system modeling

The wind conversion chain considered in this work is presented in Fig.1 consisting of a wind turbine, a PMSG, a three phase controlled rectifier connected to a DC load.

0.1 Wind profil

The wind speed is modeled in the deterministic form by a sum of several harmonics:

$$V_w(t) = 10 + 0.2sin(0.1074t) + 2sin(0.2665t) + sin(1.2930t) + 0.2sin(3.6645t) \quad (1)$$

0.2. Wind turbine

Wind turbine is applied to convert the kinetic energy of wind to mechanical torque and rotate the generator. The output power of the turbine is given by the following equation [7]:

$$P_w = \frac{\rho A V_w^3}{2} \quad (2)$$

$$\text{With } P_w = \frac{1}{2}\rho A V_w^3 \text{ and } \lambda = \frac{R\Omega_m}{V_w}$$

$P_w(W)$ is the kinetic power of wind, $A(m^2)$ is the area opposed to the wind, ρ is the air density (1.2kg/m^3 under normal conditions of temperature and humidity), C_p is the power coefficient of the turbine, λ is called the relative speed, Ω_m (rad/s) is the rotational speed of the axis of the turbine.

0.3 Permanent Magnet Synchronous Generator

To reproduce the behavior of the generator during transients, we use a dynamic model of the PMSG expressed in the reference frame of Park (dq) rotating at the same speed of the rotor. Assuming that the stator windings are distributed sinusoidally and neglecting the eddy currents and hysteresis losses, electrical equations expressed in this reference are [8]:

$$v_d = -R_s i_d + L_q \omega_e i_q - L_d \frac{di_d}{dt} + e_d \quad (3)$$

$$v_q = -R_s i_q - L_d \omega_e i_d - L_q \frac{di_q}{dt} + e_q \quad (4)$$

Where: $e_d = 0V$ et $e_q = \sqrt{\frac{3}{2}}\Phi_{sf}\omega_e$ are the load voltages ($i_d = i_q = 0$), R_s is the stator resistance, L_d and L_q are the dq inductances, ω_e is the angular frequency of the electrical currents and voltages, Φ_{sf} is the magnetic flux density. For

a synchronous machine, $\omega_e = p\Omega_m$, p is the number of pole pairs. Production of the electrical energy at the output of the generator causes a braking torque which has this expression:

$$T_e = -p(\sqrt{\frac{3}{2}}\Phi_{sf} i_q + (L_q - L_d) i_d i_q) \quad (5)$$

0.4 Three phase controlled rectifier

With the aim of resolving the optimization problem we realize a maximization analysis of the generator output power which has the following expression:

$$P_g = v_a i_a + v_b i_b + v_c i_c = v_d i_d + v_q i_q \quad (6)$$

From equations (3),(4) and (5), we deduce this expression:

$$P_g = -R_s(i_d^2 + i_q^2) - \frac{1}{2}(L_d \frac{di_d^2}{dt} + L_q \frac{di_q^2}{dt}) - T_e \Omega_m \quad (7)$$

In order to deduce expression of the generator output power, we take into account the steady state in which current and speed variations are zero: $di_d/dt = di_q/dt = 0$ (A/s) and $d\Omega_m/dt = 0$ (rad/s).
Then we get the following expression of the power:

$$P_g = C_p(\frac{R\Omega_m}{V_w}) P_w - R_s(i_d^2 + i_q^2) - f\Omega_m^2 \quad (8)$$

From equation (8), we extract this new equation:

$$C_p(\frac{R\Omega_m}{V_w}) P_w - f\Omega_m^2 = -T_e \Omega_m = \sqrt{\frac{3}{2}} p \Phi_{sf} \Omega_m i_q \quad (9)$$

Now we have an expression to maximize, equation of the power (8), taking into account a constraint equation (9). There are many methods that allow us to do this, we have chosen the Lagrange multiplier which consists of specifying the Lagrange function containing both the power and the constraint, it is expessed in (10):

$$\zeta = P_g + \lambda_\zeta (C_p(\frac{R\Omega_m}{V_w}) P_w - f\Omega_m^2 - \sqrt{\frac{3}{2}} p \Phi_{sf} \Omega_m i_q) \quad (10)$$

The next step is to solve the following four derivatives, they are given with their results:

$$\frac{\partial \zeta}{\partial i_d} = 0 \Rightarrow i_d = 0 \quad (11)$$

$$\frac{\partial \zeta}{\partial \lambda_\zeta} = 0 \Rightarrow i_q = \frac{C_p(\frac{R\Omega_m}{V_w}) P_w - f\Omega_m^2}{\sqrt{\frac{3}{2}} p \Phi_{sf} \Omega_m} \quad (12)$$

$$\frac{\partial \zeta}{\partial i_q} = 0 \Rightarrow \lambda_\zeta = \frac{4R_s}{3p^2\Phi_{sf}^2}(f - \frac{P_w}{\Omega_m^2} C_p(\frac{R\Omega_m}{V_w})) \quad (13)$$

$$\frac{\partial \zeta}{\partial \Omega_m} = 0 \Rightarrow$$

$$\frac{R\Omega_m}{V_w} \frac{dC_p(\frac{R\Omega_m}{V_w})}{d\lambda} = \frac{\lambda_\zeta C_p(\frac{R\Omega_m}{V_w}) + (\lambda_\zeta + 2) f\Omega_m^2 / P_w}{\lambda_\zeta + 1} \quad (14)$$

From the first derivative equation (11), we conclude that the power P_g reaches its maximum when d component of current is zero; $i_d = 0$, and this is why an active rectifier is implemented and controlled using the Field Oriented Control (FOC). This type of control is based on forcing the d component of current i_d to zero in accordance with results of the previous analysis. Then, the electromagnetic torque is controlled directly through the current q component i_q. From equation (5) we deduce that: $T_e = -\sqrt{\frac{3}{2}} p \Phi_{sf} i_q$

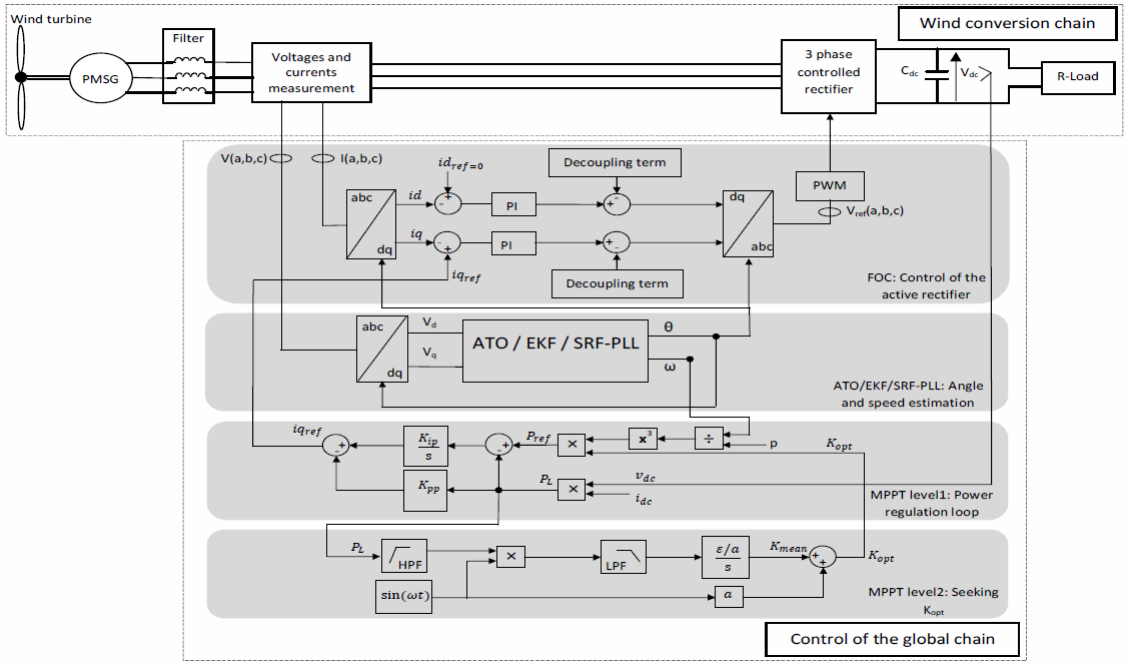

Fig. 1. Global Structure

Sensorless MPPT

As outlined in the introduction, the aim of this work is to compare three estimators used to build a sensorless MPPT strategy for the proposed WECS detailed in Fig. 1 from which we can observe that the MPPT algorithm has two levels the first is a power regulation loop generating at his output the i_{qref} for the FOC and the second is an extremum seeking system giving value of the K_{opt} . The estimators are detailed in the following.

0.5 Angle Tracking Observer

This estimator observes the projections of the output voltages of PMSG in the fixed reference frame $\alpha\beta$ using Clarcke transform. These projections are the coordinates of a vector rotating at the electrical rotor speed $\omega_e = p\Omega_m$. To estimate this speed, the observer consists in making an angle _ evolve so as cancel the algebric area of the triangle formed by the two vectors (V_α, V_β) and cos(θ), sin(θ) which is proportional to $V_\beta cos(\theta)$ - $V_\alpha sin(\theta)$.This concellation is obtained by a classical PI controller as illustrated in Fig.2, the output _ is the angle used in the direct and inverse Park transforms.

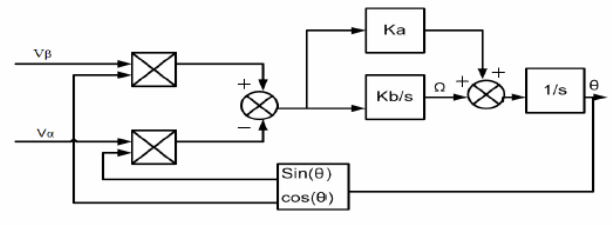

Fig. 2. Diagram of the Angle Tracking Observer

0.6 Extended Kalman Filter

0.6.1 State observation model

We consider that the velocity evolution is negligible at a sampling period to form this observation state model:

$$\begin{cases} \frac{di_d}{dt} = \frac{-u_d}{L_d} - \frac{R_s}{L_d} i_d + \frac{\omega L_q}{L_d} i_q \\ \frac{di_q}{dt} = \frac{-u_q}{L_q} - \frac{R_s}{L_q} i_q - \frac{\omega L_d}{L_q} i_d + \frac{\omega \psi_f}{L_q} \\ \frac{d\omega}{dt} = 0 \\ \frac{d\theta}{dt} = \omega \end{cases}$$

The state equation and output equation of PMSG:

$$\frac{dx}{dt} = Ax + Bu \tag{15}$$

$$y = Hx \tag{16}$$

In our case:

$$x = [i_d\ i_q\ \omega\ \theta]^T, u = [u_d\ u_q]^T, y = [i_d\ i_q]^T \tag{17}$$

From the observation state model we can deduce matrix A, B and H:

$$A = \begin{pmatrix} \frac{-R_s}{L_d} & \frac{\omega L_q}{L_d} & 0 & 0 \\ \frac{-\omega L_d}{L_q} & \frac{-R_s}{L_q} & \frac{\psi_f}{L_q} & 0 \\ 0 & 0 & 0 & 0 \\ 0 & 0 & 1 & 0 \end{pmatrix}$$

$$B = \begin{pmatrix} \frac{-1}{L_d} & 0 \\ 0 & \frac{-1}{L_q} \\ 0 & 0 \\ 0 & 0 \end{pmatrix}, H = \begin{pmatrix} 1 & 0 & 0 & 0 \\ 0 & 1 & 0 & 0 \end{pmatrix}$$

We try to estimate the state vector by considering the measurement and state noise, we consider that the sampling period is T, the first order discretized equations are:

$$x_k = f(x_{k-1}, u_{k-1}) = (I + AT)x_{k-1} + BTu_{k-1} \tag{18}$$

$$y_k = h(x_k) = Hx_k \tag{19}$$

0.6.2 EKF equations

This section describes the extended Kalman Filter which is a commonly used method to estimate the values of state variables of a dynamic system that is excited by stochastic disturbances and stochastic measurement noise. The Kalman Filter for nonlinear models is denoted the Extended Kalman Filter because it is an extended use of the original Kalman Filter. General equations of EKF are:

$$\frac{dx}{dt} = A(\hat{x})\hat{x} + Bu + K(y - \hat{y}) \tag{20}$$

$$\hat{y} = H\hat{x} \tag{21}$$

Introducing the state and measurement noise W_k and V_k respectively, non linear discrete expressions become:

$$x_k = f(x_{k-1}, u_{k-1}) + W_k \tag{22}$$

$$x_k = (I + AT)x_{k-1} + BTu_{k-1} + W_k \tag{23}$$

$$y_k = h(x_k) + V_k = Hx_k + V_k \tag{24}$$

Covariance matrices of W_k and V_k are $Q = cov(W) = E\{WW^T\}$ and $R = cov(V) = E\{VV^T\}$ respectively. Covariance matrices Q and R which have been chosen as in follows:

$$Q \models 10^{-2} \begin{pmatrix} 1 & 0 \\ 0 & 1 \end{pmatrix}, R = \begin{pmatrix} 1 & 0 \\ 0 & 1 \end{pmatrix}$$

For the discretization of the state system, we use a simple method such as Euler Method:

$$f(x_k) = x_{k-1} + \dot{x}_{k-1}\, T \tag{25}$$

So we can define the matrix F wich is ∂f/∂x as:

$$F = \begin{pmatrix} 1 - \frac{R_s}{L_d}T & \frac{L_q}{L_d}\omega T & \frac{L_q}{L_d} i_q T s & 0 \\ \frac{-L_d}{L_q}\omega T & 1 - \frac{R_s}{L_q}T & (\frac{\psi_f}{L_q} - \frac{L_d}{L_q} i_d)T & 0 \\ 0 & 0 & 1 & 0 \\ 0 & 0 & T & 1 \end{pmatrix}$$

Eventually, recursive EKF algorithm is realised through these equations:

$$\begin{aligned} &\hat{x}(k|k-1) = (I_n TA)\hat{x}(k|k) + TBu_{k-1} \\ &P(k|k-1) = FP(k|k)F^T + Q \\ &K(k|k-1) = P(k|k-1)H^T(HP(k|k-1)H^T + R)^{-1} \\ &x(k|k) = x(k|k-1) + K_k(y_k - Hx(k|k-1)) \\ &P(k|k) = P(k|k-1) - K_k HP(k|k-1) \end{aligned}$$

In these relationships, matrix K represents the Kalman gain, P the covariance state matrix and I_n is the unit matrix. In the recurrent computation relationships, the subscript index notations of type $k|k\text{-}1$ show that the respective quantities (state vectors or their covariance matrix) are computed for sample k , using the values of similar quantities from the previous sample.

0.7 SRF-PLL as angle and speed estimator

The SRF-PLL is based on aligning the output frequency with the d axis in the dq frame by using a PI controllers to force the q component voltage to zero. Referring to Fig. 3 which shows the basic structure of the SRF-PLL, the voltages in dq frame V_d and V_q are deduced from the three phase voltages V_a, V_b and V_c using Park's transform including the estimated phase angle θ :

$$\begin{bmatrix} V_d \\ V_q \\ V_0 \end{bmatrix} = \frac{2}{3} \begin{bmatrix} sin(\theta) & sin(\theta - \frac{2\pi}{3}) & sin(\theta - \frac{4\pi}{3}) \\ cos(\theta) & cos(\theta - \frac{2\pi}{3}) & cos(\theta - \frac{4\pi}{3}) \\ \frac{1}{2} & \frac{1}{2} & \frac{1}{2} \end{bmatrix} \begin{bmatrix} V_a \\ V_b \\ V_c \end{bmatrix}$$

In order to align the SRF-PLL output with d axis, the PI controllers forces the component to zero. When this output becomes in phase with the supply voltage, the PI output will be equal to ω then the angle θ can be obtained by integrating the PI output as shown.

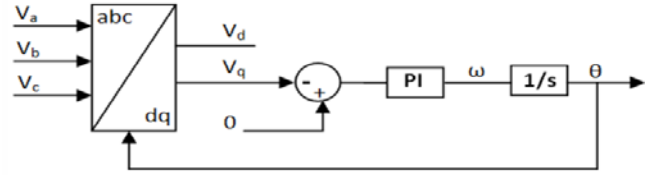

Fig. 3. Diagram of SRF-PLL

0.8 MPPT level1: Power regulation loop

We consider the expression of the turbine generated power to extract the area where are located the points of maximum power that is a curve described using the following expression:

$$(26) \qquad P_{opt} = \frac{1}{2}\rho A(\frac{R\Omega_m}{\lambda_{opt}})^3 C_{popt} = K_{opt}\Omega_m^3$$

We constructed a power control loop based on the knowledge of the optimum power value, the reference power is obtained from the estimated rotational speed and the value of the K_{opt} parameter. Structure of this loop is illustrated in Fig. 1.

0.9 MPPT level2: Seeking Kopt

For our case, we suppose that characteristics of the wind turbine are undefined so the value of K_{opt} is undetermined. In order to determine continuously this value the method of extremum seeking is implemented presenting a second level of the MPPT. As described in Fig. 1, this bloc determines an average value K_{mean} and adds a very slow sinusoidal perturbation to this value to generate the value of K_{opt} used as an input for the power control loop. Finally, we obtain variations in the average value of instantaneous power P_{inst} according to variations of the K_{opt} value at the output of a high pass filter. The low pass filter rejects the frequency of the disturbance signal at the output of multiplier. Gain a is the disturbance signal amplitude and ε adjusts the integrator gain which defines K_{mean} value.

Simulation results

As mentionned in the previous section, we consider a variable speed wind profil expressed by equation (1) and presented in Fig.4.

In order to verify the exactitude of the estimated position by the ATO we represent it with one of the three phased voltages, as showed in Fig. 5. A zoom on a short time interval is presented to better visualize the accuracy of the parameters.

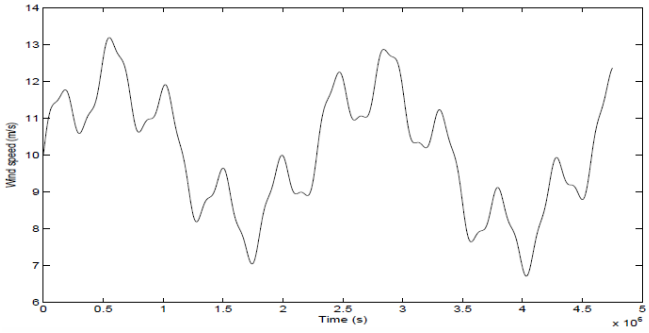

Fig. 4. variable wind speed profil

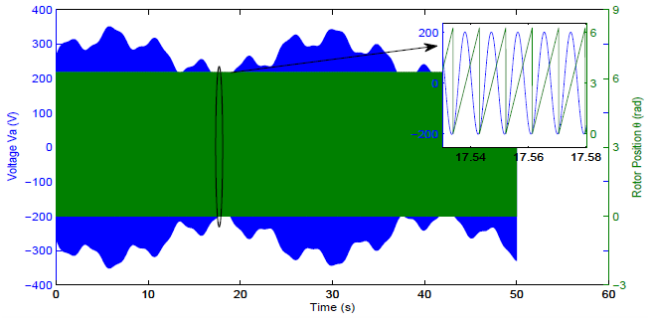

Fig. 5. Voltage Va (V) and the enstimated Rotor position (rad) by the
ATO

In Fig. 6, we present both the real speed of the generator rotor and the estimated speed using the ATO, we can deduce that the estimated speed follows correctly variations of the real speed but with a small difference in values.

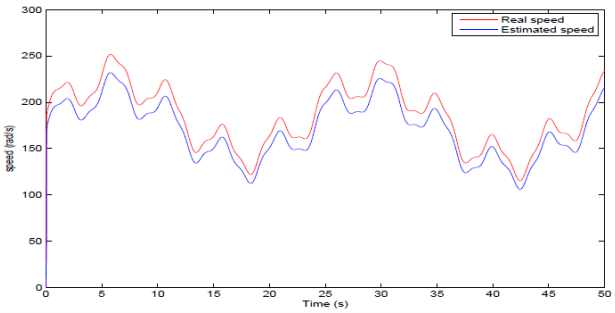

Fig. 6. Real generator speed (rad/s) and estimated generator speed (rad/s) by the ATO

The same as the ATO, we present respectively in Fig. 7 and Fig. 8 the estimated position by the EKF with one of the three phased voltages and the real generator rotor speed with the estimated speed using EKF. As can be seen the estimated speed is exactly the real speed and the precision is very good.

In Fig. 9 we present the estimated rotor speed position with the voltage Va for the third estimator the SRF-PLL. Finally, Fig. 10 illustrates the real generator rotor speed and the estimated speed using the SRF-PLL, it is clear that also the SRF-PLL gives a speed that follows perfectly the real one and we can say that the difference in values is neglicted.

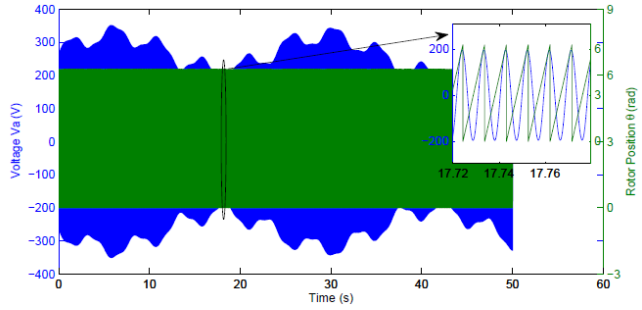

Fig. 7. Voltage Va (V) and the enstimated Rotor position (rad) by the EKF

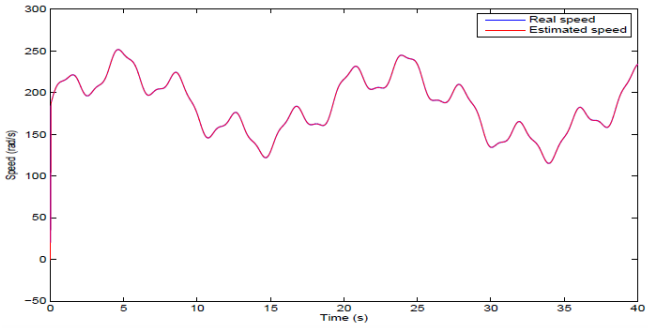

Fig. 8. Real generator speed (rad/s) and estimated generator speed (rad/s) by the EKF

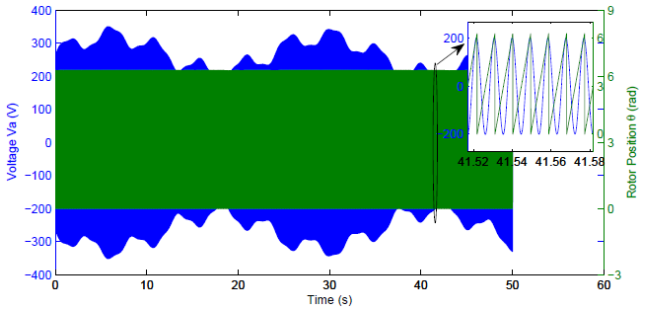

Fig. 9. Voltage Va (V) and the estimated Rotor position (rad) by the SRF-PLL

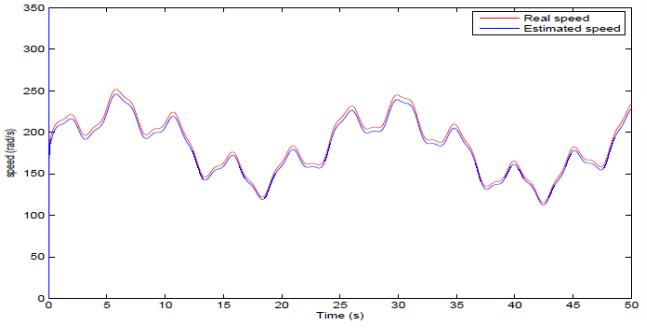

Fig. 10. Real generator speed (rad/s) and estimated generator speed (rad/s) by the SRF-PLL

Conclusion

In this paper a sensorless MPPT strategy was applied to a variable wind speed WECS composed of a wind turbine, a PMSG and an active rectifier connected to a DC load. The complete structure is presented in Fig. 1. In order to justify the use of the FOC, an analysis of the power maximizition was realized. The main aim of this work is to compare three estimators used to build the mechanical sensorless MPPT, the ATO, the EKF and the SRF-PLL. Matlab-Simulink simulation results shows the performances of these estimators and their effectiveness in variable wind speed profils, comparing performance of the three estimator it appears that the EKF gives the most accurate estimation of both the generator rotor speed and angle. Finally Advantages and disadvantages of the three estimators are summarized in Table 1.

Table 1. Advantages and Disadvantages of the three estimators

Estimator	Advantages	Disadvantages
ATO	• Simplicity of implementation • Ability to calculate estimation errors	• Requires a fast calculation unit • Less effective for rapid variations
EKF	• Ability to predict the error correction parameters of the sensors and the model • Ability to determine the average error of the estimated parameters • Validity for nonlinear modeling	• The covariance of the error (estimation accuracy) does not necessarily converge • High computational cost due to expensive matrices used in calculations
SRF-PLL	• Good performance under distroted voltage conditions • Low cost	• Slow response during transient and sensitive to frequency fluctuation and unbalanced voltage

***Authors**: Ph.D. student Amina Echchaachouai , Prof. S. El Hani, Department of Electrical engineering, ENSET Rabat, Mohammed V University, Rabat, Morocco, email: amina.echchaachouai@um5s.net.ma, Prof. A. Hammouch, National Center for Scientific and Technical Research, Rabat, Morocco*

REFERENCES

[1] Polinder H., van der Pijl F. F. A., De Vilder G. J., Tavner P. J.: Comparison of direct-drive and geared generator concepts for wind turbines, IEEE Trans. Energy Conversion, vol. 21, no. 3, pp. 725–733, Sep. 2006.

[2] Yan Y., Wang S., Xia C., Wang H., Shi T. : Hybrid Control Set-Model Predictive Control for Field-Oriented Control of VSI-PMSM, IEEE Transactions on Energy Conversion, Volume: 31, Issue: 4, Dec. 2016.

[3] Tan Y., Moase W., Manzie C., Nesic D., Mareels I. : Extremum seeking from 1922 to 2010, Proc.of the 29th Chinese Control Conference, pp. 14-26. 2010.

[4] Auger F., Mansouri-Toudert O., Chibah A.: Design of advanced resolver-to-digital converters, proc. Electrimacs conf., 2011.

[5] Gowda M., Ali W. h., Cofie P., Fuller J. : Design and Digital Implementation
of Controller for PMSM Using Extended Kalman Filter, Circuits and Systems, 4, pp. 489-497, Published Online Dec. 2013.

[6] Gonzlez-Esp F., FigureS E., Garcer G.: An Adaptive Synchronous-Reference-Frame Phase-Locked Loop for Power Quality Improvement in a Polluted Utility Grid, IEEE Transactions on Industrial Electronics, Volume: 59 , Issue: 6, pp. 2718-2731. 2012.

[7] Infield D., Freris L. : Les energies renouvelables pour la production d'electricite, Techniques et Ingenierie, Dunod/Dunod lusine nouvelle, 2013.

[8] Bhende C. N., Mishra S.,Senior Member, IEEE, Malla S. G.: Permanent Magnet Synchronous Generator-Based Standalone Wind Energy Supply System, IEEE Tansactions on Sustainable Energy, vol. 2, no. 4, pp. 361–373, October. 2011.